The Effects of Klapskate Hinge Position on Push-off Performance: A Simulation Study

HAN HOUDIJK, MAARTEN F. BOBBERT, JOS J. DE KONING, and GERT DE GROOT

Institute for Fundamental and Clinical Human Movement Sciences, Faculty of Human Movement Sciences, Vrije Universiteit, Amsterdam, THE NETHERLANDS

ABSTRACT

HOUDIJK, H., M. F. BOBBERT, J. J. DE KONING, and G. DE GROOT. The Effects of Klapskate Hinge Position on Push-off Performance: A Simulation Study. *Med. Sci. Sports Exerc.*, Vol. 35, No. 12, pp. 2077–2084, 2003. **Purpose:** The introduction of the klapskate in speed skating confronts skaters with the question of how to adjust the position of the hinge in order to maximize performance. The purpose of this study was to reveal the constraint that klapskate hinge position imposes on push-off performance in speed skating. **Method:** For this purpose, a model of the musculoskeletal system was designed to simulate a simplified, two-dimensional skating push off. To capture the essence of a skating push off, this model performed a one-leg vertical jump, from a frictionless surface, while keeping its trunk horizontally. In this model, klapskate hinge position was varied by varying the length of the foot segment between 115 and 300 mm. With each foot length, an optimal control solution was found that resulted in the maximal amount of vertical kinetic and potential energy of the body's center of mass at take off (W_{eff}). **Results:** Foot length was shown to considerably affect push-off performance. Maximal W_{eff} was obtained with a foot length of 185 mm and decreased by approximately 25% at either foot length of 115 mm and 300 mm. The reason for this decrease was that foot length affected the onset and control of foot rotation. This resulted in a distortion of the pattern of leg segment rotations and affected muscle work (W_{mus}) and the efficacy ratio (W_{eff}/W_{mus}) of the entire leg system. **Conclusion:** Despite its simplicity, the model very well described and explained the effects of klapskate hinge position on push off performance that have been observed in speed-skating experiments. The simplicity of the model, however, does not allow quantitative analyses of optimal klapskate hinge position for speed-skating practice. **Key Words:** SPEED SKATING, SPORTS EQUIPMENT, LOCOMOTION, MUSCULO-SKELETAL MODEL, BIOMECHANICS

Klapskates have become the custom equipment in speed skating. In contrast to the conventional skates, in which the shoe is rigidly fixed to the blade, klapskates incorporate a hinge between shoe and blade, which allows the skater to rotate his foot independent of the skate blade (6,15). The introduction of the klapskate in the international skating community was followed by an overwhelming and almost instantaneous improvement in speed-skating performance. Currently, skaters and manufacturers are faced with the question of how to optimally adjust their klapskates to maximally benefit from its advantages. The most important properties to adjust and optimize might be the position of the hinge between shoe and blade (1,8). The ratio between the moment arm of the calf muscles and the maximal moment arm of the ground (ice) reaction force with respect to the ankle joint can be manipulated to shift the gear ratio of the calf muscles and influence their mechanical performance (5).

Address for correspondence: H. Houdijk, Vrije Universiteit Amsterdam, Faculty of Human Movement Sciences, Van der Boechorststraat 9, 1081 BT Amsterdam, The Netherlands; E-mail: h_houdijk@fbw.vu.nl.
Submitted for publication March 2003.
Accepted for publication August 2003.

0195-9131/03/3512-2077
MEDICINE & SCIENCE IN SPORTS & EXERCISE®

DOI: 10.1249/01.MSS.0000099085.84271.AB

As a matter of fact, it has been hypothesized that the major advantage of klapskates over conventional skates should be attributed to such a difference in gear ratio (8,9). It was shown that, despite the common belief that skaters should suppress plantar flexion with conventional skates, skaters with both conventional skates and klapskates plantar flexed their ankle and rotated their foot at the end of the push off (9). With conventional skates, however, the foot had to rotate around the tip of the long skate blade, whereas with klapskates the foot rotated around the hinge of the skate. It was argued that this difference in the location of the center of foot rotation accounted for the increase in work per stroke that was generated with klapskates compared with conventional skates (9).

Field experiments to further investigate the effect of klapskate hinge position on push-off performance have, unfortunately, not resulted in a conclusive understanding of this effect (1,8). These field experiments, however, have several limitations that can obscure these effects. Measurements of speed-skating mechanics on an ice rink contain noise, which may conceal the small but relevant effects of changing hinge position beneath the ball of the foot. In addition, it is questionable whether skaters can easily adjust their technique to different hinge positions and it is unclear how much training a skater needs to accustom his technique to each new hinge position.

An alternative approach that does not suffer from these limitations is the use of an optimal control model of the musculoskeletal system. In such a simulation model, prop-

erties of the musculoskeletal system and skate can be manipulated systematically. Furthermore, the neural control of the musculoskeletal system can be optimized to realize the maximum performance with each hinge position. In addition, the underlying mechanical effects of changing hinge position can be analyzed in more detail and can be traced back to the mechanical response of individual muscles.

Recently, an optimal control model was developed and used to investigate the mechanical characteristics of a push off in speed skating (4). In that study, the speed-skating push off was modeled as a one-leg vertical jump from a frictionless surface. With this model, the effect of submaximal activation, the specific initial skating position, the absence of surface friction, and the effect of maintaining a horizontal trunk position on push-off performance were investigated. Additionally, it was investigated what the effect was of increasing the "effective" foot length of a barefooted jumper (the distance between the ankle joint and the metatarsophalangeal joints) to the "effective" foot length imposed by currently used klapskates. It was shown that with such a model the salient features of a push off in speed skating could be captured and explained well in a qualitative way and hence provide insight in how the mechanical constraints of speed skating affect push-off performance, although it should be realized that the model was too simple to replicate the speed-skating push in great quantitative detail.

In the present study, this optimal control model of the push off in speed skating was used to investigate the effect of klapskate hinge position on push-off performance. Model results were used to reveal the constraints that klapskate hinge position imposes on push-off performance of the model. Subsequently, the qualitative results of the model were compared with previous experimental results and used to explain the experimentally observed effects of klapskate hinge position on push-off mechanics in speed skating.

METHODS

We used a simplified, two-dimensional optimal control model of the speed-skating push off. With this model, the push off in speed skating was simplified to a constrained one-leg vertical jump. This model has recently been described and evaluated by Bobbert et al. (4) and will briefly be discussed below.

The simulation model, which calculates the motion of body segments corresponding to muscle stimulation-time input, was based on the model presented previously by Van Soest et al. (17,18). The model for speed skating consisted of four rigid segments representing the foot, shank, and thigh of the push-off leg and a rigid HATL-segment, representing the head, arms, trunk, and swing leg (Fig. 1). These segments were interconnected through hinge joints, representing ankle, knee, and hip. In the initial position, the full foot was in contact with the surface. The heel could be lifted from the surface at any time after the start of the simulation. In that case, the foot rotated around its distal end. The distal end of the foot segment, hence, represented the hinge of the klapskate. The anthropometric parameters

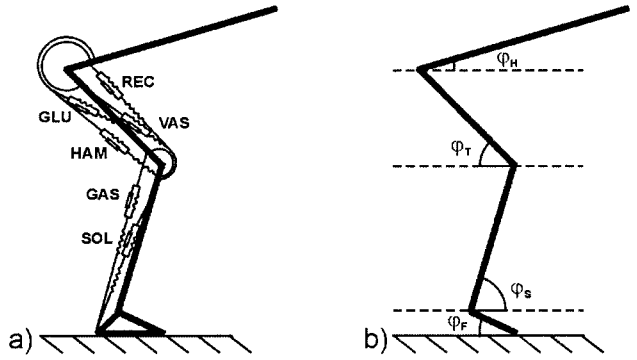

FIGURE 1—a. Schematic drawing of the musculoskeletal model. The model consists of four rigid body segments: foot, lower leg, upper leg, and HATL, and six leg muscles: m. gluteus, hamstrings, mm vasti, m. rectus femoris, m. soleus, and m. gastrocnemius. b. Definition HATL (ϕ_H), thigh (ϕ_T), shank (ϕ_S), and foot (ϕ_F) angle.

of the model were arbitrarily based on an average Dutch male (17,18). The parameters of the skeletal submodel are shown in Table 1.

The segments were actuated by six Hill-type muscle-tendon complexes (MTC), which represented the major leg muscles: m. soleus, m. gastrocnemius, mm vasti, m. rectus femoris, m. gluteus maximus, and hamstrings. The independent input of the model was muscle stimulation (STIM). Initially STIM of each muscle was set such that static equilibrium was maintained. Subsequently, STIM of each muscle was allowed to switch to its maximal level once and had to maintain this level until take off.

A change in klapskate hinge position was modeled as a change in the length of the foot segment of the model. In this simulation experiment, foot length was varied systematically between 115 and 300 mm, the latter representing the "effective" foot length of a skater with conventional skates. These foot lengths were equivalent to hinge positions located 33–279 mm anterior to the ankle joint. In the current klapskates the hinge is located approximately 170 mm anterior to the ankle joint (9) and provides an effective foot length of approximately 205 mm. Changing foot length in the model was accompanied by an adjustment of the initial foot angle to ensure that the initial height of the ankle joint remained constant.

To reproduce as many of the specific characteristics of the speed-skating push off as possible in the two-dimensional model, several constraints were imposed on the model: 1) The model was placed in an initial position derived from experimental data on speed skating (9). 2) The maximal level of stimulation was set to half of the full activation, to account for the fact that speed skaters perform multiple push offs during their races, in contrast to a single maximum height jump. Because stimulation level affects the rate of CA^{2+} influx to the muscle, this resulted in a slower rate of force development, whereas maximal force could still be attained. Consequently, push-off duration was elongated. 3) The friction between foot and surface in fore-aft direction was set to zero, to model the interface between blade and ice. Hence, the foot could move freely in horizontal direction. 4) A penalty was set on the rotation of the HATL

TABLE 1. Parameters of the skeletal model.

	Length (mm)	d_{cm} (mm)	Mass (kg)	I_{cm} (kg·m^{-2})	φ_o (°)
Foot	185–300	120	1.243	0.010	21.5–73.3
Shank	458	260	3.537	0.068	63.4
Thigh	485	275	8.472	0.209	39.3
HATL	500	220	69.020	3.902	22.3

d_{cm}, position of the center of mass relative to the caudal end of the segment; I_{cm}, moment of inertia relative to the segment's center of mass; φ_o, initial segment angles. Note that foot length and foot angle are varied to change hinge position.

segment from the initial position. This penalty value was introduced into the optimization criterion to account for the fact that speed skaters have to maintain a horizontal trunk position in order to minimize the opposing force from air friction.

The stimulation switching times of the six muscles in the model were optimized to find maximal push-off performance. In speed skating, skaters aim to maximize mechanical power output, which is the product of work per stroke and stroke frequency. However, it has been demonstrated that in the different skating events, skaters regulate velocity predominantly by regulating stroke frequency, work per stroke being more or less constant. In addition, a high correlation has been demonstrated between work per stroke and skating performance (13). Hence, we defined push-off performance in speed skating as the amount of external work per stroke (12,14). In our model, this is equivalent to the amount of vertical kinetic and potential energy of the body's center of mass at take off, and will be referred to as effective energy (W_{eff}). The effective energy depends on the work generated by the muscles (W_{mus}) and the ratio at which muscle work is converted into effective energy, i.e., the efficacy ratio (W_{eff}/W_{mus}) (2). The remainder of the muscle work is lost into the rotational kinetic energy of the body segments. The optimization problem was solved using a genetic optimization algorithm (16). For each foot length tested, muscle stimulation was reoptimized.

The result of a simulation of a push off with currently used klapskates and, for comparison, experimental data of a speed-skating push off are shown in Figure 2.

RESULTS AND DISCUSSION

In this study, an optimal control model of a simplified speed-skating push off was used to gain insight into the effects of klapskate hinge position on push-off performance. Below, we will first investigate and discuss the constraint that foot length (or klapskate hinge position) imposes on the push-off performance of the model. Subsequently, it will be discussed how these simulation results compare to and explain previous experimental findings. Finally, the limitations of this simulation approach will be discussed.

Despite the complex dynamics of the musculoskeletal system, the relation between foot length and effective energy (W_{eff}) appeared to be smooth with a clear optimum (Fig. 3). Effective energy steadily increased with foot length up to the optimum foot length of 185 mm. Beyond 185 mm, effective energy decreased steeply and subsequently leveled off. The maximum effective energy of 278 J was reached with the foot length of 185 mm (Table 2). Effective energy

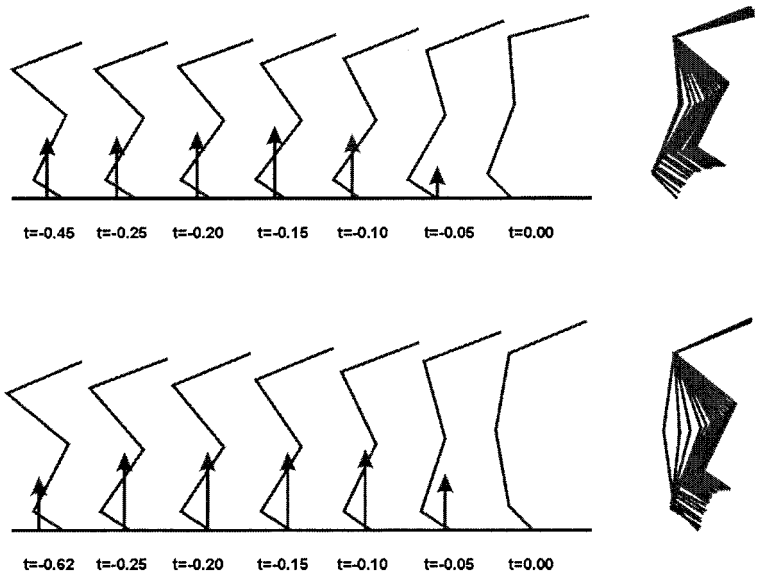

FIGURE 2—Comparison of experimental data of a speed-skating push off with klapskates (hinge at 205 mm, upper panel) and simulation data (lower panel). Experimental data are viewed in a moving reference plane fitted through hip, knee, and ankle of the skater. The leftmost stick figures depict the initial body configuration before the onset of the push off. The rightmost stick figure depicts the body configuration at take off. In each stick figure, the ground reaction force vector is represented with its origin at the center of pressure. In the rightmost column, the configuration of the skeletal system has been plotted at 20-ms time intervals with the hip joint used as origin. Note that a hyperextension of the knee in the model occurs as no special provisions were included to satisfy this anatomical constraint.

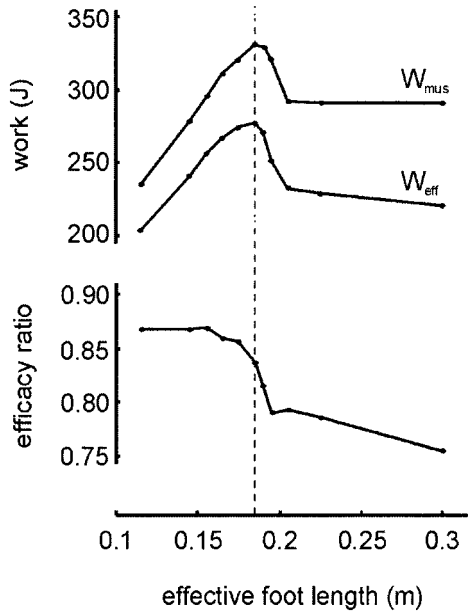

FIGURE 3—Effective energy (W_{eff}), total muscle work (W_{mus}), and efficacy ratio (W_{eff}/W_{mus}) as a function of foot length. Maximum effective energy was obtained with an effective foot length of 185 mm (*vertical dashed line*).

decreased by 27% when foot length was maximally reduced and by 21% when foot length was increased to a length approaching the effective foot length with conventional skates.

The effective energy that was generated by the model depends on the work generated by the muscles (W_{mus}) and on the ratio at which muscle work is converted into vertical kinetic energy and potential energy of the body's center of mass, i.e., the efficacy ratio (W_{eff}/W_{mus}). As can be seen in Figure 3, muscle work reached a maximum with the foot length of 185 mm, just as the effective energy did. However, although the decrease in effective energy with shorter foot lengths could totally be attributed to a decrease in muscle work, the decrease in effective energy with larger foot lengths was due to both a decrease in muscle work and a decrease in the efficacy ratio. With a foot length of 300 mm, 70% of the decrease in effective energy was due to a decrease in muscle work and 30% to a decrease in the efficacy ratio.

Work generated by the individual muscles, arranged by the joint about which they exert an extension moment, is shown in Figure 4 (left panels). Table 2 shows the contribution of the individual muscles to total muscle work at optimal foot length and to the decrease in muscle work at foot lengths surrounding the optimum and both extremes. Clearly, it can be seen that differences in work of the plantar flexors accounted for the largest part of the differences in total muscle work. Work generated by the plantar flexors decreased considerably with foot lengths below and above optimum. Work done by the knee extensors gradually decreased with increasing foot length from 115 to 205 mm. In contrast, work output of the hip extensors increased with increasing foot length from 115 to 195 mm, after which it leveled off.

Work produced by an individual muscle depends on the distance of shortening, the shortening velocity, and active state. These variables were analyzed to find the cause of the changes in muscle work. Figure 4 shows the force-length diagram (middle panels) and velocity-length diagram (right panels) of the contractile elements of the three monoarticular joint extensors (i.e., m. gluteus maximus, mm vasti, and m. soleus), which were the main work generators. The area under the force-length diagram represents contractile element work. The results for a push off with optimum foot length, 185 mm, and for a push off with a foot length of 165 mm and 205 mm are shown to clarify why muscle work changes with foot length.

As already pointed out, changes in foot length affected most the work output of the plantar flexors. The reduction in work output with foot lengths above optimum (185 mm) was due to an increase in shortening velocity and a reduction in the range of shortening. The reduction in work output

TABLE 2. Work (J) related parameters for a 185-mm foot length (absolute values; bold print), foot lengths surrounding the optimum and both extremes (expressed relative to 185 mm; Δ).

	Foot Length (mm)						
	115 Δ	**165 Δ**	**175 Δ**	**185**	**195 Δ**	**205 Δ**	**300 Δ**
W_{eff}	−74	−10	−3	**278**	−30	−45	−57
W_{mus}	−96	−20	−10	**331**	−10	−39	−40
Efficacy ratio	0.03	0.02	0.02	**0.84**	−0.05	−0.04	−0.08
W_{glu}	−23	−8	−5	**102**	11	3	1
W_{ham}	−14	−4	−3	**44**	7	−6	−4
W_{vas}	14	0	0	**107**	−3	−13	−7
W_{rec}	−3	2	1	**4**	−1	5	−1
W_{sol}	−50	−8	−4	**51**	−10	−13	−16
W_{gas}	−20	−1	1	**24**	−14	−14	−14
W_{hip}	−43	−15	−7	**175**	21	12	20
W_{knee}	35	11	4	**59**	−17	−42	−40
W_{ankle}	−89	−16	−7	**97**	−13	−10	−20
$Trans_{hip}$	−6	−2	1	**29**	2	16	22
$Trans_{knee}$	24	9	3	**−51**	−14	−33	−32
$Trans_{ankle}$	−19	−7	−4	**22**	11	17	11

W_{eff}, effective energy; W_{mus}, total muscle work; W_{glu} to W_{gas}, work output of individual muscles; W_{hip} to W_{ankle}, individual net joint work; $Trans_{hip}$ to $Trans_{ankle}$, net transport of energy between the individual joints. Positive energy transport indicates transport to the joint.

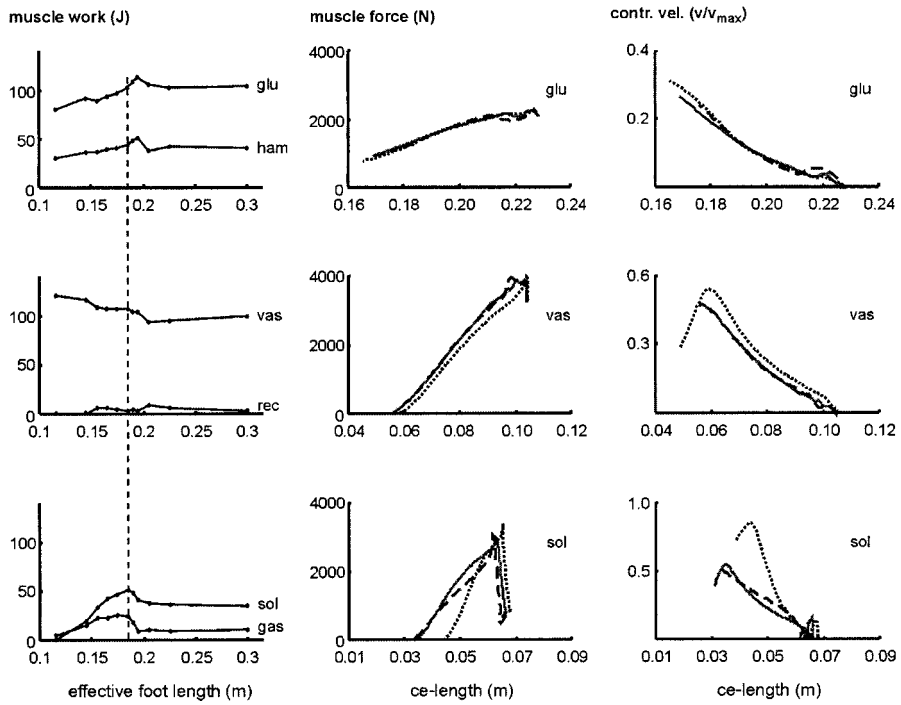

FIGURE 4—Left panels: muscle work as a function of foot length. Muscles are arranged by the joint about which they exert an extensor torque. The *dashed line* indicates the optimal effective foot length of 185 mm. Middle panels: force-length diagrams of the contractile elements (CE) of the three monoarticular leg muscles, for the push off with the foot length of 165 mm (*dashed*), 185 mm (*solid*), and 205 mm (*dotted*). The surface below the curves represents muscle work. Right panels: muscle shortening velocity (expressed relative to maximal unloaded shortening velocity; v/v_{max}) versus length of the contractile elements for the three monoarticular leg muscles. Similar foot lengths as used in the middle panels are displayed.

with foot lengths below optimum was due to a change in active state. Below optimal foot length, the onset of STIM of the plantar flexors was delayed with decreasing foot length (Table 3). Consequently, the plantar flexors initially shortened without developing force and, hence, without generating work. The slight reduction in work of the mm vasti with increasing foot length could be ascribed to an increase in shortening velocity and occurred despite an increase in the shortening distance. Work done by the m. gluteus increased with foot length due to an increase in the shortening distance. However, with foot lengths beyond 195 mm, shortening velocity also increased, which reduced muscle force and, hence, counteracted the effect of increasing shortening distance.

The features that are described here for the monoarticular joint extensors applied, for the largest part, equally to their biarticular synergists. Hence, it can be summarized that with foot lengths above optimum, muscle work decreased as a result of increasing contraction velocities of all muscles. With foot lengths below optimum, muscle work decreased because of a delayed activation of the plantar flexors and, to a lesser extent, because of a smaller range of shortening of the hip extensors. Now, how can these effects on muscle contraction conditions and work be explained?

TABLE 3. Stimulation onset times (s) of all muscles for optimum foot length, the foot lengths surrounding the optimum, and both extremes.

	Foot Length (mm)						
	115	**165**	**175**	**185**	**195**	**205**	**300**
Glu	0.37	0.05	0.05	0.05	0.05	0.05	0.05
Ham	0.23	0.27	0.31	0.33	0.33	0.30	0.30
Vas	0.05	0.13	0.16	0.17	0.17	0.23	0.15
Rec	0.49	0.36	0.46	0.49	0.53	0.32	0.45
Sol	0.60	0.38	0.38	0.36	0.37	0.30	0.34
Gas	0.54	0.40	0.39	0.34	0.32	0.33	0.45

As has been described previously (4,8,10), "effective" foot length imposes an important constraint on the timing of foot rotation. Rotation of the foot starts when the net ankle torque, mainly generated by the plantar flexor muscles, exceeds the couple of the reaction forces that act on the foot (i.e., the net joint reaction force and ground reaction force). Initially, the foot is at rest with the heel on the floor. Hence, as the sum of moments has to be zero, the center of pressure of the ground reaction force under the foot is such that the couple of the reaction forces equals the net ankle torque. When the net ankle torque starts to rise, the center of pressure under the foot will shift forward, and the balance of both torques is remained. Only when the center of pressure under the foot reaches the end of the foot segment, and hence cannot shift further forward, does the ankle torque exceed the couple of reaction forces and does the foot start to rotate. The effective foot length, hence, determines when the foot will start to rotate in response to a given ankle torque and reaction forces.

When the foot length of the model was increased above 185 mm, the maximal moment arm of the couple of reaction forces exceeded a critical length. Above this length, the maximal ankle torque of the fully activated plantar flexor muscles was not sufficient to initiate rotation of the foot in response to the existing reaction forces at the start of the push off (Fig. 5). Foot rotation was inevitably delayed until the hip and knee joint torques decreased and the reaction forces dropped. The resultant delay in foot rotation was responsible for the reduced push-off performance (2,8,10). In a multi-segment leg system, the action of each segment influences the kinematics of every other segment due to the

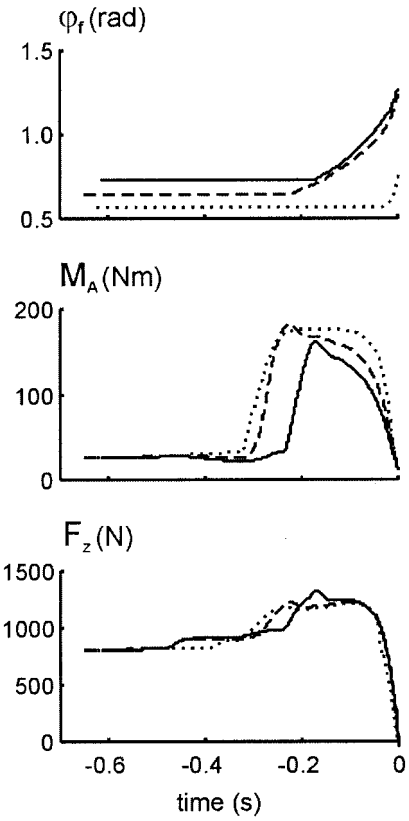

FIGURE 5—Time histories of foot angle (ϕ_f), net ankle torque (M_A), and ground reaction force (F_z) for the push off with a foot length of 165 mm (*dashed*), 185 mm (*solid*), and 205 mm (*dotted*). Note that with a foot length of 205 mm, the maximal ankle torque is not sufficient to initiate foot rotation. In that case foot rotation only starts after F_z has dropped.

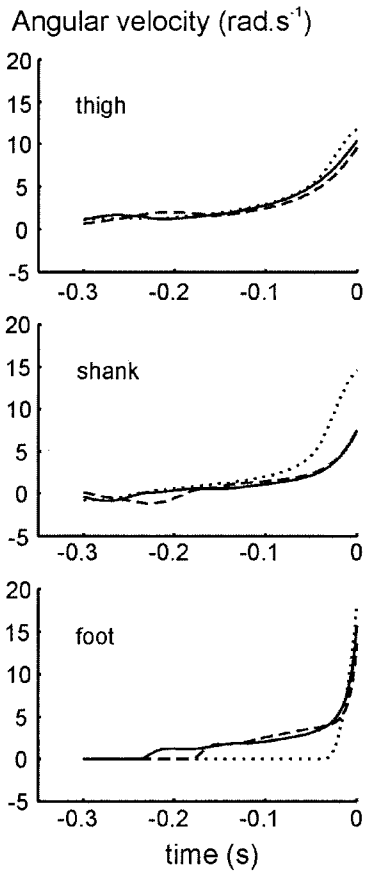

FIGURE 6—Time histories of angular velocity of thigh, shank, and foot, for the push off with a foot length of 165 mm (*dashed*), 185 mm (*solid*), and 205 mm (*dotted*). Note that with a foot length of 205 mm the pattern of leg segment rotations became distorted and peak angular velocities increased.

dynamical coupling between them (11,19). Hence, the delay in foot rotation affected the kinematics of all leg segments. In this case, the sequential pattern of leg segment rotations became distorted. Shank rotation started early, immediately with thigh rotation, while the foot followed after a large delay. In addition, all segment angular velocities and joint extension velocities increased (Fig. 6). This resulted in an increase of muscle shortening velocities and ultimately the reduction of muscle work. Additionally, the efficacy ratio dropped, because a larger portion of the muscle work ended up as rotational kinetic energy of the leg segments.

When the foot length was reduced below 185 mm, it became easier to rotate the foot. The shorter the foot length, the less the plantar flexor torque had to be built up to initiate foot rotation in response to the existing reaction forces. This then introduced the next problem: foot rotation might be initiated too early. When the plantar flexor muscles were stimulated as early with a short foot as with the optimal 0.185-m foot, a premature foot rotation would occur. Such a premature rotation of the foot would probably result in a take off with incomplete extension of knee and hip joint, as was recently demonstrated (2). The optimization routine figured out that a delay in the activation of the plantar flexor muscles was less detrimental than an early take off, despite a reduction in active state during the first part of their range of shortening and, hence, a reduction in their work output.

So, we can conclude that foot length constrains push-off performance because it affects the control of foot rotation. The foot length (and thus klapskate hinge position) that yields maximal work per stroke needs to allow a proper timing of foot rotation in response to the extension of knee and hip joint. It will, hence depend strongly on the length and configuration of the other leg segments and the strength of the leg muscles. The simulation results showed that only a limited range of foot lengths allows for the required timing and maximal work output.

In previous field experiments, in which the effects of hinge position on the kinematics and kinetics of the speed-skating push off was investigated (1,8,9), three consistent effects were found when the hinge was moved anteriorly: 1) the onset of foot rotation was delayed; 2) the angular displacement as well as peak angular velocity of knee and hip joint increased; and 3) work done about the knee joint decreased. The delay in the onset of foot rotation and the increase in knee and hip extension and extension velocity that have been observed when the hinge is moved anteriorly were confirmed and accounted for in this simulation study. However, the reduction in joint work about the knee, as observed in the experimental studies is not directly evident from the presented results. In fact, in our model long foot lengths primarily affected the work output of the plantar flexors instead of the knee extensor muscles (Table 2). Are

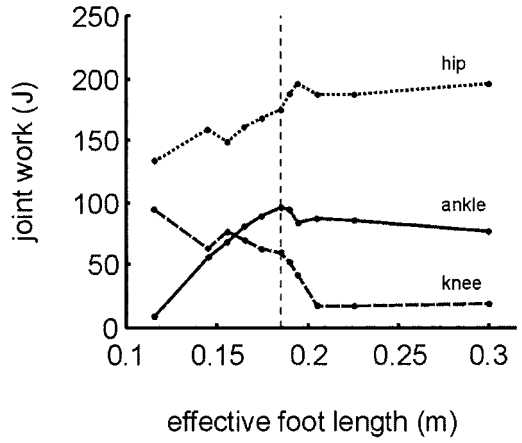

FIGURE 7—Net joint work as a function of foot length. Work output about the ankle (*solid*), knee (*dashed*), and hip (*dotted*) are shown. The foot length of 185 mm is indicated by the *vertical dashed line*.

these results in contradiction with the reduction of the work output about the knee joint that has been observed in skaters?

Net joint work, calculated as the time integral of the product of net joint torque and joint angular velocity, is shown in Figure 7 as a function of foot length. It can be seen that, in accordance with the results from skating experiments, work done about the knee joint dropped with foot lengths above optimum. This reduction in knee work was not due to a reduction in the work output of the knee extensor muscles, but could be explained from the energy-transporting capacity of biarticular muscles (3,12). The work output of the knee extensor muscles did not emerge about the knee joint but was transported by the hamstrings to the hip where it appeared as net hip work and transported by the gastrocnemius to the ankle where it appeared as net ankle work. This magnitude of the transport of muscle work was affected by foot length (Table 2). Partly as a result of the increased extension velocity of the knee, the biarticular gastrocnemius and hamstrings generated a higher moment of force around the knee joint during the entire range of knee extension, which increased the transport of energy to both ankle and hip. These data stress the hypothetical nature of joint work (12). Although net joint power or work can be accessed relatively easily in human experiments, this does not directly shed light on its source.

It can be concluded that, despite the simplicity of the model, three main effects of the position of the center of foot rotation on push off mechanics in speed skating can be reproduced and explained with this model. This qualitative correspondence between experimental and simulation data strengthens our belief that the general effects of effective foot length on push off mechanics as demonstrated by the model are valid for speed skating.

Despite the qualitative agreement between model and experimental results, no quantitative conclusions should be drawn from this study. The model was not designed to represent the skating push off in a quantitative detailed manner but merely to establish the mechanical constraint that hinge position imposes on push of performance. It is therefore not surprising that the optimal hinge position predicted by the model (0.185 m) differs considerably from the hinge position that is currently favored by elite skaters (ca. 0.205 m). A number of limitations of the model can contribute to this difference: 1) In the model, gravity acts in the plane of the push-off leg, whereas in reality, this force will act at an angle to this plane toward the end of the push off. 2) The model lacks provisions to limit hyperextension of the knee, which results in a deviation between the kinematics of the model and the real speed-skating push off at the end of the push off. However, it is not known how this constraint is handled passively or actively in the body. The choice to ignore this constraint will probably result in an exaggerated effect of foot length compared with reality, because joint angular velocities rise unlimited. However, it should be realized that imposing an additional penalty on knee hyperextension can only reduce performance further. 3) Maximal muscle stimulation was arbitrarily set to 50% of its real maximum to account for the repetitive and therefore submaximal nature of the movement. As described before, this will predominantly affect the rate of force development. It has been shown for jumping that this does not affect the general effect of hinge position (7), but it can affect the quantitative results. 4) Finally, it can be wondered whether maximal work per stroke is the only relevant optimization criterion for speed skating. Maximal performance might also depend on minimizing metabolic cost (i.e., high mechanical efficiency). However, the validity of models describing the metabolic cost of muscle contraction is yet questionable. Thus, such a criterion is difficult to incorporate. Considering all of these limitations, a conclusive quantitative statement on the optimal hinge position for speed skating cannot be given.

CONCLUSION

In conclusion, we have found that this simplified model of the speed-skating push off can reproduce and explain the effects of klapskate hinge position on push-off performance in speed skating. Klapskate hinge position affects the control of foot rotation and therewith the work output of the entire leg system. Obviously, klapskate hinge position is an important parameter for skaters to consider. The optimum hinge position for each individual skater, however, will probably depend on many factors as for instance body build, technique, fatigue, etc., and might therefore be difficult to determine.

This study was supported by the Technology Foundation STW, applied science division of NOW, and the technology program of the Ministry of Economic Affairs.

REFERENCES

1. ALLINGER, T. L., and R. W. MOTL. Experimental vertical jump model used to evaluate the pivot location in klap speed skating. *J. Appl. Biomech.* 16:142–156, 2000.
2. BOBBERT, M. F., and A. J. VAN SOEST. Why do people jump the way they do? *Exerc. Sport Sci. Rev.* 29:95–102, 2001.
3. BOBBERT, M. F., P. A. HUIJING, and G. J. VAN INGEN SCHENAU. An estimation of power output and work done by the human triceps surae muscle-tendon complex in jumping. *J. Biomech.* 19:899–906, 1986.
4. BOBBERT, M. F., H. HOUDIJK, J. J. DE KONING, and G. DE GROOT. From a one-legged vertical jump to the speed skating push-off: a simulation study. *J. Appl. Biomech.* 18:28–45, 2002.
5. CARRIER, D. R., N. C. HEGLUND, and K. D. EARLS. Variable gearing during locomotion in the human musculoskeletal system. *Science* 265:651–653, 1994.
6. DE KONING, J. J., H. HOUDIJK, G. DE GROOT, and M. F. BOBBERT. From biomechanical theory to application in top sports: the klapskate story. *J. Biomech.* 33:1225–1229, 2000.
7. HOUDIJK, H., M. F. BOBBERT, and J. J. DE KONING. The effect of forefoot length on vertical jumping performance. *Med. Sci. Sports Exerc.* 32:S340, 2000.
8. HOUDIJK, H., J. J. DE KONING, M. F. BOBBERT, and G. DE GROOT. How klapskate hinge position affects push-off mechanics in speed skating. *J. Appl. Biomech.* 18:292–305, 2002.
9. HOUDIJK, H., J. J. DE KONING, G. DE GROOT, M. F. BOBBERT, and G. J. VAN INGEN SCHENAU. Push-off mechanics in speed skating with conventional skates and klapskates. *Med. Sci. Sports Exerc.* 32:635–641, 2000.
10. HOUDIJK, H., A. J. WIJKER, J. J. DE KONING, M. F. BOBBERT, and G. DE GROOT. Ice friction in speed skating: can klapskates reduce ice frictional loss? *Med. Sci. Sports Exerc.* 33:499–504, 2001.
11. PUTNAM, C. A. A segment interaction analysis of proximal-to-distal sequential segment motion patterns. *Med. Sci. Sports Exerc.* 23:130–144, 1991.
12. VAN INGEN SCHENAU, G. J. From rotation to translation: constraints on multi-joint movements and the unique action of bi-articular muscles. *Hum. Mov. Sci.* 8:301–337, 1989.
13. VAN INGEN SCHENAU, G. J., G. DE GROOT, and R. W. DE BOER. The control of speed in elite female speed skaters. *J. Biomech.* 18:91–96, 1985.
14. VAN INGEN SCHENAU, G. J., R. W. DE BOER, and G. DE GROOT. On the technique of speed skating. *Int. J. Sport Biomech.* 3:419–431, 1987.
15. VAN INGEN SCHENAU, G. J., G. DE GROOT, A. W. SCHEURS, H. MEESTER, and J. J. DE KONING. A new skate allowing powerful plantar flexions improves performance. *Med. Sci. Sports Exerc.* 28:531–535, 1996.
16. VAN SOEST, A. J., and L. J. R. CASIUS. The merits of a parallel genetic algorithm in solving hard optimization problems. *J. Biomech. Eng.* 125:141–146, 2003.
17. VAN SOEST, A. J., P. A. HUIJING, and M. SOLOMONOW. The effect of tendon on muscle force in dynamic isometric contractions: a simulation study. *J. Biomech.* 28:801–807, 1995.
18. VAN SOEST, A. J., A. L. SCHWAB, M. F. BOBBERT, and G. J. VAN INGEN SCHENAU. SPACAR: a software subroutine package for simulation of the behavior of biomechanical systems. *J. Biomech.* 25:1219–1226, 1992.
19. ZAJAC, F. E., and M. E. GORDON. Determining muscle's force and action in multi-articular movement. In: *Exercise and Sport Science Reviews*, K. Pandolf (Ed.). Baltimore: Williams & Wilkins, 1989, pp. 187–230.